Level structure and spin-orbit effects in semiconductor nanorod dots

C. L. Romano,[1,2] S. E. Ulloa,[1] and P. I. Tamborenea[2]

[1]*Department of Physics and Astronomy and Nanoscale and Quantum Phenomena Institute, Ohio University, Athens, Ohio 45701-2979*

[2]*Department of Physics, University of Buenos Aires, Ciudad Universitaria, Pab. I, C1428EHA Buenos Aires, Argentina*

(Dated: November 1, 2004)

We investigate theoretically how the spin-orbit Dresselhaus and Rashba effects influence the electronic structure of quasi-one-dimensional semiconductor quantum dots, similar to those that can be formed inside semiconductor nanorods. We calculate electronic energy levels, eigen-functions, and effective g-factors for coupled, double dots made out of different materials, especially GaAs and InSb. We show that by choosing the form of the lateral confinement, the contributions of the Dresselhaus and Rashba terms can be tuned and suppressed, and we consider several possible cases of interest. We also study how, by varying the parameters of the double-well confinement in the longitudinal direction, the effective g-factor can be controlled to a large extent.

PACS numbers: 73.21.La, 73.21.-b, 72.25.-b
Keywords: spin-orbit coupling, Dresselhaus effect, Rashba effect, quantum dots

arXiv:cond-mat/0411003 v1 29 Oct 2004

I. INTRODUCTION

In recent years, much of the research in semiconductor physics has been shifting towards *spintronics*,[1,2] the novel branch of electronics in which the information is carried, at least in part, by the spin of the electrons. The electron spin might be used in the future to build quantum computing devices combining logic and storage based on spin-dependent effects in semiconductors. In order to achieve this goal, much study has been devoted recently to magnetic and optical[3] properties of semiconductors quantum dots[4,5] and quantum wells.[6] One of the most popular spin-based devices was proposed by Datta and Das.[7] Improvements to the original design have been proposed recently by Egues et al.[8,9] The Datta-Das device makes use of the Rashba spin-orbit coupling[10,11] in order to perform controlled rotations of the spins of electrons passing through the channel of a field-effect transistor (FET), thus creating a spin-FET. The Rashba term is the manifestation of the spin-orbit interaction in quasi-one-dimensional (quasi-1D) semiconductor nanostructures lacking *structural* inversion symmetry. Additionally, the lack of *bulk* inversion symmetry enables another spin-orbit term in the electronic Hamiltonian, the Dresselhaus term,[12] which is also taken into account in the spin-FET design introduced in Ref. [9].

The influence of the Rashba and Dresselhaus Hamiltonians in quantum dots (QD) has recently been treated in a number of theoretical works. The most-often studied geometry is that of quasi-two-dimensional dots with parabolic confinement in the plane.[13,14,15] On the other hand, there is a growing interest and experimental progress in another type of quantum dots defined inside quasi-1D structures called nanorods or nanowhiskers.[16] In these structures, additional confinement in the longitudinal direction can be introduced with great precision, thereby allowing the formation of quasi-1D heterostructures, such as multiple quantum dots[17,18] and dot superlattices.[19] Nanorods can be grown out of numerous semiconductor materials. Their lateral widths can be controlled by selecting the size of the gold nanoparticles which are used to catalyze their growth and can be made as small as 3 nm.[20] Recently, the transport properties of these nanorod dots have been measured and the gated control of the number of electrons in them has been demonstrated.[18]

Motivated by this experimental progress, we study theoretically the electronic structure of quasi-1D coupled double dots including spin-orbit effects. This type of dot systems has also attracted interest in the field of quantum control of orbital wave functions due to their simplicity and tunability.[21,22,23,24] As we will see here they are also well-suited for applications involving control of the spin degrees of freedom since they allow a great deal of control over the Rashba and Dresselhaus Hamiltonians. In this paper we study the influence of the Rashba and Dresselhaus spin-orbit Hamiltonians on the electronic structure of quasi-1D QDs, akin to those formed in semiconductor nanorods. Our emphasis on the spin-orbit interaction is obviously motivated by the current widespread interest in developing spintronic applications, which require a detailed understanding of the dynamics of the spin degree of freedom in semiconductor nanostructures.

Let us denote by x and y the two transversal and by z the longitudinal direction of a quasi-1D nanorod, and let us call $V_z(z)$ the confining potential that defines a pair of coupled QDs along the nanorod. The laterally-confining potentials $V_x(x)$ and $V_y(y)$ are crucial in the determination of the Rashba and Dresselhaus Hamiltonians and we consider different combinations of these potentials which can arise in our elongated geometry. We calculate the energy spectra and the wave functions by exact numerical diagonalization of the total Hamiltonian and analyze how the energy levels and the effective g-factor change as the Rashba and Dresselhaus couplings are modulated by varying the lateral confining potentials. Furthermore,

we study the effect of varying the size of one of the dots and the width of the central barrier between them. Since the strength of the spin-orbit interaction varies greatly among semiconductor compounds, we look at several materials such as GaAs, InSb, GaSb, and InAs. Finally, we investigate the effective spin $\langle S_z \rangle$ as a function of the strength of the Rashba-like term for all the eigenfunctions of InSb with two different geometries.

The quantization along different directions results in peculiar spin-momentum dependence. This in turn results in SO effects that depend strongly on the symmetries of the lateral confinement potentials. As such, the observation of SO spin splittings, as we will see, is directly attributable to asymmetry of the confinement and provides an interesting probe of built-in strain fields and/or unbalanced composition gradients.

We organize the paper as follows. In Sec. II we introduce the effective one-dimensional Hamiltonian and list the simplified forms it takes depending on the choice of confinement potentials. In Sec. III we present the results for the energy levels including either the Dresselhaus or the Rashba term. In Sec. IV we study the effective g-factor and the expectation value of the z-component of the spin as a function of the strength of the Rashba term for different semiconductors and eigenstates. In Sec. V we provide a discussion and conclusion.

II. THE ONE-DIMENSIONAL HAMILTONIAN

We start with the complete Hamiltonian for a three-dimensional semiconductor structure in the absence of magnetic field,

$$H = \frac{p^2}{2m^*} + V(\mathbf{r}) + H_D + H_R, \tag{1}$$

where m^* is the conduction-band effective mass, $\mathbf{p}$ is the momentum, $V(\mathbf{r})$ is the confinement potential, and H_D and H_R are the general Dresselhaus and Rashba Hamiltonians.[25] Here we follow the current practice of calling Rashba terms those spin-orbit contributions to the Hamiltonian that arise due to the structural inversion asymmetry of the nanostructure, as opposed to the Dresselhaus terms which come from the bulk inversion asymmetry of the III-V semiconductors. Integrating out the x and y variables, we obtain the following effective one-dimensional Hamiltonian:

$$H_{1d} = \frac{p_z^2}{2m^*} + V_z(z) + H_{1dD} + H_{1dR}, \tag{2}$$

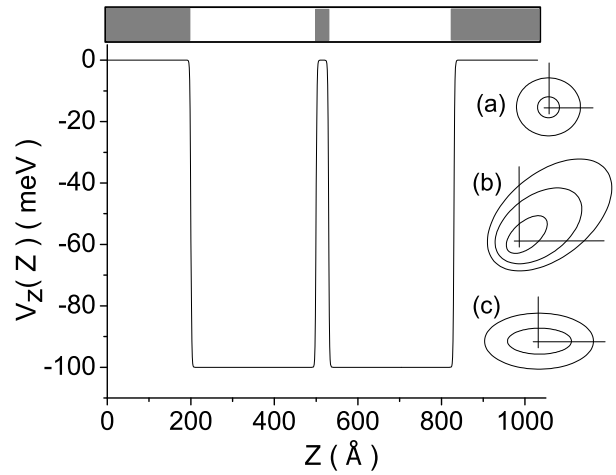

FIG. 1: Potential-energy profile and schematic drawing of two Al/InSb coupled nanorod quantum dots. For InSb-based systems we take a well height of 100 meV, and for Al/GaAs, 220 meV. In this example, the QD width is 300 Å and barrier width 30 Å, with smoothly changing barriers over a width of a few angstroms. The drawings (a)-(c) illustrate the lateral confinement geometries described in the text.

$$\begin{aligned} H_{1dD} &= \frac{\gamma_D}{\hbar^3}\{\sigma_x \langle p_x \rangle \left(\langle p_y^2 \rangle - p_z^2\right) - \sigma_y \langle p_y \rangle \left(\langle p_x^2 \rangle - p_z^2\right) \\ &+ \sigma_z p_z \left(\langle p_x^2 \rangle - \langle p_y^2 \rangle\right)\}, \end{aligned} \tag{3}$$

$$\begin{aligned} H_{1dR} &= \frac{\gamma_R}{\hbar}\{\sigma_x \left(\left\langle \frac{\partial V_y}{\partial y} \right\rangle p_z - \frac{\partial V_z}{\partial z} \langle p_y \rangle\right) - \\ &- \sigma_y \left(\left\langle \frac{\partial V_x}{\partial x} \right\rangle p_z - \frac{\partial V_z}{\partial z} \langle p_x \rangle\right) + \\ &+ \sigma_z \left(\left\langle \frac{\partial V_x}{\partial x} \right\rangle \langle p_y \rangle - \left\langle \frac{\partial V_y}{\partial y} \right\rangle \langle p_x \rangle\right)\}, \end{aligned} \tag{4}$$

where σ_i, $i = x, y, z$, are the Pauli matrices, H_{1dD} is the one-dimensional Dresselhaus term, and H_{1dR} is the Rashba-like term enabled by the inversion asymmetry of the laterally confining potentials V_x and V_y. γ_R and γ_D are parameters that depend on the materials. The averages $\langle \ldots \rangle$ are taken over the lowest-energy wavefunctions of the laterally confining potentials as we assume small nanorod widths. In Table I we present the parameters used in our calculations for different semiconductor materials. An example of the confining potential in the longitudinal direction, $V_z(z)$, is shown in Fig. 1, along with a schematic drawing of the nanorod QDs.

We now list four different possibilities for the confining potentials $V_x(x)$ and $V_y(y)$, based on the degree of symmetry of the structure. The Dresselhaus and Rashba Hamiltonians simplify considerably due to the fact that, in the absence of a magnetic field, the eigenstates can be chosen real, and therefore, expectation values of the momentum are zero.[26] The four cases are (see Fig. 1(a)-(c) for schematic drawings of the potentials in the first three cases):

(a) Circular: $V_x(x), V_y(y)$ have inversion symmetry

about the origin and are equal, $V_x(x) = V_y(y)$:

$$H_{SO} = H_{1dD} + H_{1dR} = 0, \tag{5}$$

yields no SO contributions.

(b) $V_x(x), V_y(y)$ have no inversion symmetry but are equal, $V_x(x) = V_y(y)$:

$$H_{SO} = H_{1dD} + H_{1dR} = \frac{\gamma_R}{\hbar}\left\langle \frac{\partial V_x}{\partial x}\right\rangle p_z(\sigma_x - \sigma_y), \tag{6}$$

so that only Rashba terms are present.

(c) Elliptical: $V_x(x), V_y(y)$ are inversion symmetric functions and different, $V_x(x) \neq V_y(y)$:

$$H_{SO} = H_{1dD} + H_{1dR} = \frac{\gamma_D}{\hbar^3}\sigma_z p_z\left(\langle p_x^2\rangle - \langle p_y^2\rangle\right), \tag{7}$$

results in only Dresselhaus terms.

(d) $V_x(x), V_y(y)$ have no inversion symmetry and are different, $V_x(x) \neq V_y(y)$:

$$H_{SO} = H_{1dD} + H_{1dR} = \frac{\gamma_D}{\hbar^3}\sigma_z p_z\left(\langle p_x^2\rangle - \langle p_y^2\rangle\right) + \frac{\gamma_R}{\hbar}p_z\left(\sigma_x\left\langle\frac{\partial V}{\partial y}\right\rangle - \sigma_y\left\langle\frac{\partial V}{\partial x}\right\rangle\right), \tag{8}$$

represents the most general case and both Rashba and Dresselhaus contributions are present.

For the calculation of the effective g-factor we introduce a weak magnetic field along the z-direction. The field is chosen small so that the $x-y$ orbital wave functions are not perturbed significantly. Thus, we only add a Zeeman term to the Hamiltonian, $H_Z = \frac{\mu_B}{2} g_0 B\sigma_z$, where μ_B is the Bohr magneton, $\mathbf{B}$ is the magnetic field, and g_0 is the electron g-factor as per Table I. To calculate the energy levels and eigenfunctions, we expand the total Hamiltonian on a basis set of 300 wave functions of the quantum box of size L, i.e. $\phi_{n,s}(z) = \sqrt{\frac{2}{L}} sin(\frac{n\pi z}{L})\chi(s)$, where $\chi(s)$ is the spin function, and diagonalize it numerically without further approximations. The size L of the box is such that the whole double-dot structure is enclosed in the box, including the barriers on the sides of the dots and as such is irrelevant in the final eigenstates. We should notice that the geometry of the dots that we study here includes widths of 2-5 nm, while the most common nanorod widths in experiments are of the order of tens of nm. However, as we mentioned above, there are no experimental limitations to reducing the nanorod width to values we consider here. Smaller widths allow us to explore the basic physics and control of electronic wave functions with only one relevant lateral energy sublevel. Moreover, notice that typical charge depletion induced by the free surfaces further reduces the effective width of the nanorods, making them more 1D-like. A final comment is that the incorporation of additional transverse levels in the nanorod is straightforward, but results in systems of coupled differential equations.

III. ENERGY LEVELS

We present results for the energy levels in cases (b) and (c), i.e. with only Rashba and Dresselhaus terms present, respectively. The general case (d) does not present qualitatively different features from (b) or (c) and therefore we concentrate here on the simpler cases. For case (b) we fix the strength of the Rashba term by giving the structural electric field $\langle\frac{\partial V}{\partial x}\rangle$. For case (c), we use as confining potentials in the lateral directions two harmonic-oscillator potentials with different frequencies: $V_q(q) = \frac{1}{2}m^*\omega_q^2 q^2$, $q = x, y$. These potentials have associated characteristic lengths $\ell_q = \sqrt{\hbar/m^*\omega_q}$.

TABLE I: Parameters for semiconductors[25]

Parameter	GaAs	GaSb	InAs	InSb
$m^* = m/m_0$[27]	0.067	0.041	0.0239	0.013
γ_R[28] (A^2)	5.33	33	110	500
γ_D[27] (meV/A^3)	24	187	130	220
g_0	−0.44	−7.8	−15	−51

In Fig. 2 we plot the two lowest energy levels for the InSb QDs taking $\langle\frac{\partial V}{\partial x}\rangle = 0.5\,\text{meV/ Å}$ for case (b), and $\ell_x = 50\,\text{Å}$, $\ell_y = 20\,\text{Å}$ for case (c). The indices on the horizontal axis denote the inclusion of different terms in the Hamiltonian. The figure shows how the energy levels of H_0 (indices 1 and 4) are changed by the inclusion of a Rashba contribution H_{1dR} (case (b), index 2), and of a Dresselhaus contribution H_{1dD} (case (c), index 5), without magnetic field. With a weak magnetic field we have total Hamiltonians $H_0 + H_{1dR} + H_Z$ (index 3) and $H_0 + H_{1dD} + H_Z$ (index 6). We have carried out analogous calculations for the semiconductors quoted in Table I and the results were qualitatively similar to the ones shown here. The main general conclusion is that the effect of H_{1dR} is always stronger than that of H_{1dD} for the chosen parameters, which are representative of possible experimental situations. We note that the Rashba and Dresselhaus terms do not remove the spin degeneracy (as expected from the Kramers degeneracy in the absence of

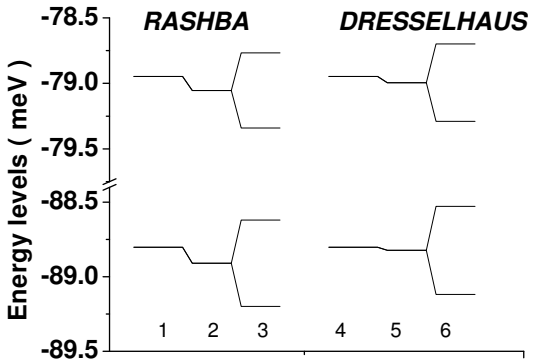

FIG. 2: Ground-state and first-excited-state energy levels of the InSb nanorod QDs shown in Fig. 1. We compare the eigenenergies of (1,4) $H_0 = \frac{P_z^2}{2m^*} + V_z(z)$ to those of (2) $H_0 + H_{1dR}$, (5) $H_0 + H_{1dD}$, (3) $H_0 + H_{1dR} + H_Z$, and (6) $H_0 + H_{1dD} + H_Z$. $B = 0.2$T.

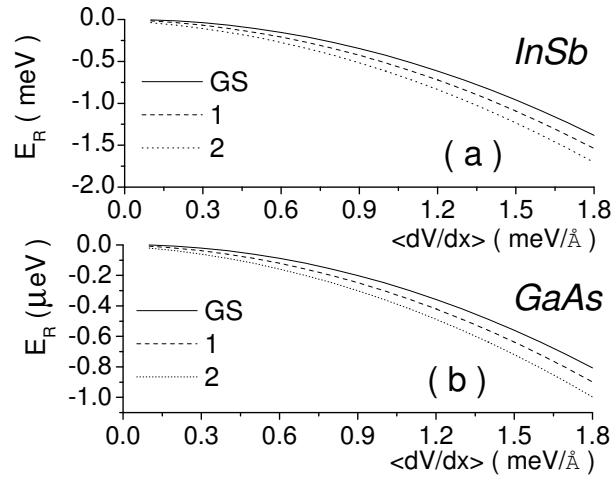

FIG. 3: Contribution of the Rashba term to the energy levels of InSb (a) and GaAs (b) QDs as a function of $\langle \frac{\partial V}{\partial x} \rangle$. GS: Ground state, 1 and 2: first and second excited states, respectively. Notice effect is much smaller in GaAs (energy given in μeV), as anticipated.

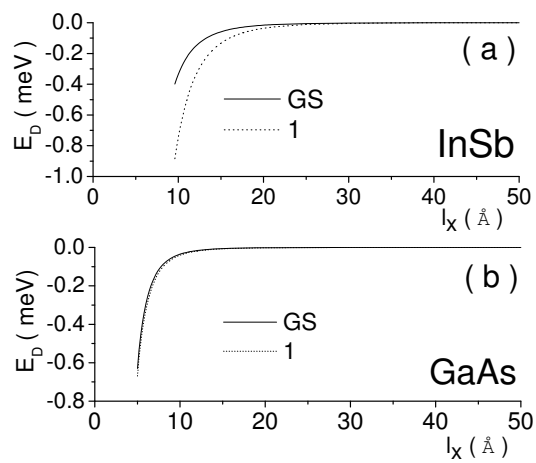

FIG. 4: Contribution of the Dresselhaus term to the energy levels of InSb as a function of ℓ_x for the ground state (GS) and the first excited state (1) for $\ell_y = 50$ Å. Level splitting in GaAs is barely visible on the same scale as in InSb.

magnetic field) but that they simply shift the levels downwards, the strength of the shifts being controlled by the parameters $\langle \frac{\partial V}{\partial x} \rangle$ for Rashba and ℓ_x and ℓ_y for Dresselhaus. For the parameters chosen here the Rashba shift is of the order of 0.1meV for InSb and 0.1μV for GaAs while the Dresselhaus shift is of the order of 0.01meV for InSb and 0.01μV for GaAs.

As can be seen in Fig. 3 the energy shift produced by the H_{1dR} varies quadratically with the structural electric field $\langle \frac{\partial V}{\partial x} \rangle$. In Fig. 4 we show how the energy levels vary in case (c) as a function of ℓ_x for the two lowest-energy states for fixed $\ell_y = 50$ Å. The functional dependence here is also parabolic. This suggests that the spin-orbit corrections to the energy levels could be calculated fairly accurately with second-order perturbation theory. We performed the second-order perturbative calculation in the case with Rashba Hamiltonian, with a small magnetic field applied (0.1 T) in order to work with non-degenerate perturbation theory. A comparison between the exact and second-order energies shows, for example, a difference of 17% for $\langle \frac{\partial V}{\partial x} \rangle = 1.5\,\mathrm{meV/Å}$, and increasing differences for larger Rashba fields, as expected. These results agree qualitatively with those of Ref. [14] for quasi-2D circular dots, where differences of up to 30% between the results of exact calculations and of second-order perturbation theory have been found.

IV. EFFECTIVE g-FACTOR

The small magnetic field $\mathbf{B} = 0.1\mathrm{T}\,\mathbf{z}$ breaks the spin degeneracy of the ground state and allows the calculation of the effective g-factor (g^*) as a function of $\langle \frac{\partial V}{\partial x} \rangle$ (case (b)) for GaAs, InSb, InAs and GaSb. In the figures we report normalized g-factors:

$$\frac{g^*}{g_0} = \frac{(E_2 - E_1)}{\frac{\mu_B B g_0}{2}}, \tag{9}$$

where E_1 and E_2 are the Zeeman-split ground-state levels. Figure 5 shows the results for case (b) (i.e. with only Rashba contributions) as a function of $\langle \frac{\partial V}{\partial x} \rangle$. The decreasing trend of g^* is qualitatively similar for all the materials but the magnitude of this Rashba effect varies greatly among them. The decrease of the g^* is strongest for InSb and weakest for GaAs.

We now examine what happens to g^* when one modifies the features of the longitudinal potential $V_z(z)$, such as the barrier width w and the size of the QDs (so far we have taken $L_{QD1} = L_{QD2} = 300$ Å). In Fig. 6(a) we show g^* for $w = 30, 130$, and 330 Å as a function of $\langle \frac{\partial V}{\partial x} \rangle$. We increase the barrier width but reducing at the same time the sizes of the two QDs so that the to-

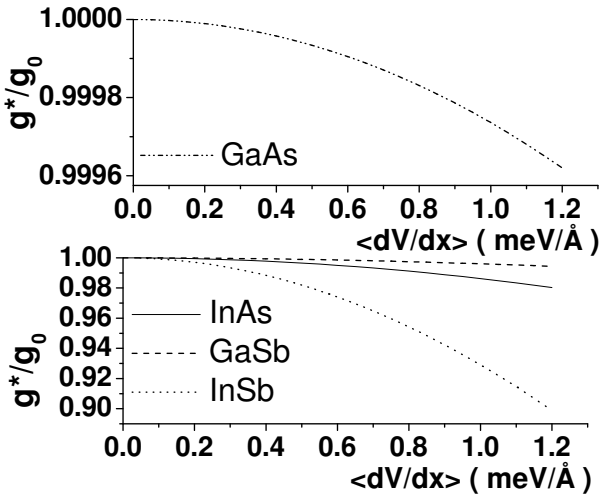

FIG. 5: Effect of the Rashba Hamiltonian on the effective g-factor. g^*/g_0 for the ground state for different semiconductors as a function of $\langle \frac{\partial V}{\partial x} \rangle$.

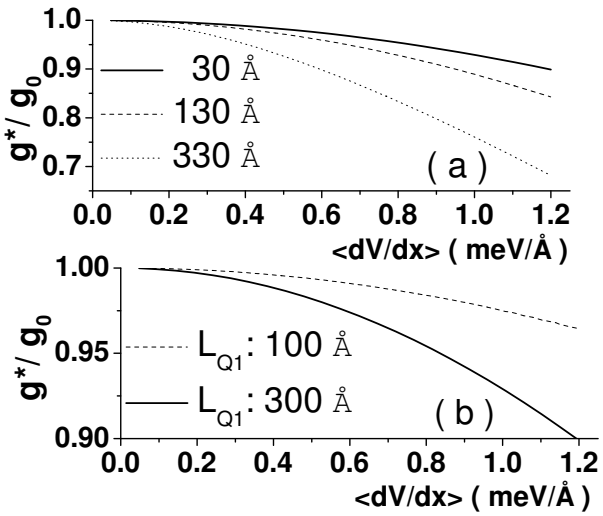

FIG. 6: Normalized effective g-factor for the ground state of InSb structures with Rashba Hamiltonian. (a) For different barrier widths $w = 30, 130, 330$Å. (b) For different sizes of the QDs. Asymmetric case: $L_{QD1} = 100$ Å and $L_{QD2} = 500$ Å; symmetric case $L_{QD1} = L_{QD2} = 300$ Å.

tal size of the structure remains constant at 630 Å. We note that increasing w leads gradually to having two uncoupled QDs and to a stronger variation of g^*. In Fig. 6(b) we set $w = 30$ Å and change the QDs' sizes. We take $L_{QD1} = 100$ Å and $L_{QD2} = 500$ Å in one case, and $L_{QD1} = L_{QD2} = 300$ Å in the other. We observe here that the *symmetric* potential produces a stronger variation of g^* than the *asymmetric* one.

We look at these symmetric and asymmetric structures in more detail, and calculate the expectation value $\langle S_z \rangle$ as a function of $\langle \frac{\partial V}{\partial x} \rangle$ for InSb dots and for the four lowest pairs of states (Zeeman doublets). Again a magnetic field

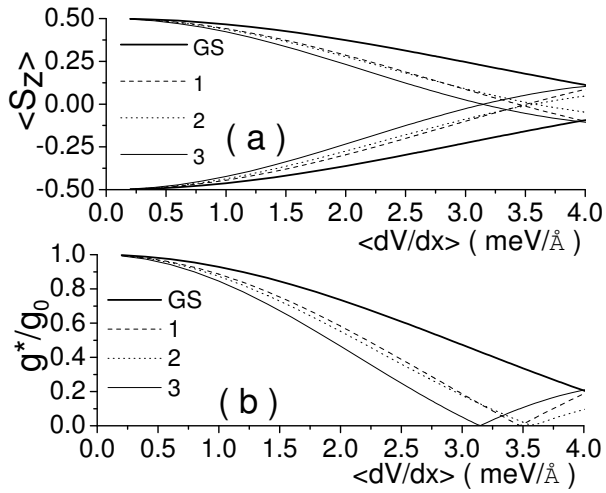

FIG. 7: Mean value of S_z and effective g-factor for InSb systems with symmetric $V_z(z)$ (two equal dots with $L_{QD1} = L_{QD2} = 300$ Å). (a) $\langle S_z \rangle$ as a function of $\langle \frac{\partial V}{\partial x} \rangle$ for the four lowest-energy doublets (pairs of Zeeman-split states). (b) g^*/g_0 for the same states.

$\mathbf{B} = 0.1$T is included. As expected, $\langle S_z \rangle = \pm\frac{1}{2}$ in the absence of $\langle \frac{\partial V}{\partial x} \rangle$. Figure 7 shows the results for a symmetric structure with $L_{QD1} = L_{QD2} = 300$ Å and Fig. 8 for an asymmetric one with $L_{QD1} = 100$ Å and $L_{QD2} = 500$ Å. The symmetric case shows a crossing in $\langle S_z \rangle$ (Fig. 7(a)) while the asymmetric one does not (Fig. 8(a)). Using this information we recalculate the effective g-factor for the first four pairs of eigenstates for the symmetric (Fig. 7(b)) and asymmetric (Fig. 8(b)) structures. The effective g-factor, given here by the difference in $\langle S_z \rangle$ values for every Zeeman pair, vanishes at the crossing of $\langle S_z \rangle$. This vanishing of g^* is a potentially useful effect in spintronics applications, as it can be achieved as a function of the potentially adjustable Rashba parameter $\langle \frac{\partial V}{\partial x} \rangle$. It is interesting to note how different spatial asymmetry, introduced by the confinement potential along z (i.e. different size dots), has strong effect on g^*, and results in a finite value even at large Rashba fields.

V. CONCLUSIONS

We have studied how the spin-orbit Rashba and Dresselhaus terms modify the electronic structure of nanorod quasi-one-dimensional double quantum dots. We have solved the problem by numerical diagonalization of the total Hamiltonian for varying confining potentials, in the lateral as well as in the longitudinal directions. The main conclusions of our work are the following:
(1) For our system, the Rashba and Dresselhaus Hamiltonians shift downwards the energy levels but do not break the spin degeneracy of the electronic levels in the absence of an external magnetic field (as prescribed by the Kramers degeneracy.)

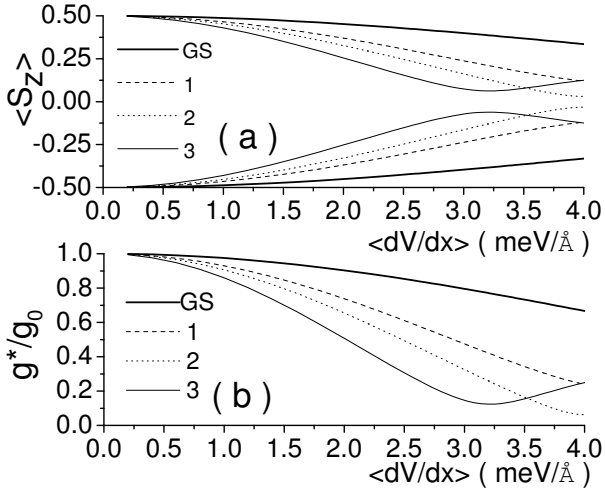

FIG. 8: Same as Fig. 7 for asymmetric $V_z(z)$ with $L_{QD1} = 100$ Å and $L_{QD2} = 500$ Å

(2) The Rashba effects are in general stronger than the Dresselhaus effects, but the latter are not negligible in general either.
(3) Changing the strength of the spin-orbit terms, which is done by changing the lateral confinement length ℓ_x or ℓ_y in the case of Dresselhaus or the structural electric field $\left\langle \frac{\partial V}{\partial x} \right\rangle$ in the case of Rashba, results in energy levels that vary nearly quadratically with the control parameter. This indicates that the SO corrections to the energy levels are close to the second-order corrections in perturbation theory. We verified this result by comparing the exact and the perturbatively calculated energies.
(4) By changing the strength of the Rashba term, the size of the central barrier, and the size and symmetry of the two QDs, it is possible to control the value of the effective g-factor, which determines the Zeeman splitting. In particular, it is possible to make the effective g-factor equal to zero.

Acknowledgments

We acknowledge support from the CMSS Program at Ohio University, Proyectos UBACyT 2001-2003 and 2004-2007, Fundación Antorchas, ANPCyT grant 03-11609, and NSF-CONICET through a US-Argentina-Brazil collaboration grant NSF 0336431. P.I.T. is a researcher of CONICET.

[1] G. A. Prinz, Science **282**, 1660 (1998).
[2] S. A. Wolf *et al.*, Science **294**, 1488 (2001). *Semiconductor Spintronics and Quantum Computation* D. D. Awschalom, D. Loss, N. Samarth (eds) (Springer, Berlin, 2002).
[3] D. Gammon and D. G. Steel, Physics Today, October 2002, pp. 36-41.
[4] M. B. Tavernier *et al.*, Phys. Rev. B **68**, 205305 (2003); **90**, 146801 (2003).
[5] D. Loss and D. P. DiVincenzo, Phy. Rev. A **57**, 120 (1998).
[6] K. J. Goldammer *et al.*, J. Vac. Sci. Technol. **B 16(3)**, May/June (1998).
[7] S. Datta and M. Das, Appl. Phys. Lett. **56**, 665 (1990).
[8] J. C. Egues, G. Burkard, and D. Loss, Appl. Phys. Lett. **82**, 2658 (2003).
[9] J. Schliemann, J. C. Egues, and D. Loss, Phys. Rev. Lett. **90**, 146801 (2003).
[10] E. I. Rashba, Sov. Phys. Solid State **2**, 1109 (1960).
[11] Y. A. Bychkov and E. I. Rashba, JETP Lett. **39**, 78 (1984); J. Phys. C **17**, 6039 (1984).
[12] G. Dresselhaus, Phys. Rev. **100**, 580 (1955).
[13] M. Governale, Phys. Rev. Lett. **89**, 206802 (2002).
[14] E. Tsitsishvili, G. S. Lozano, A. O. Gogolin, Phys. Rev. B **70**, 115316 (2004).
[15] C. F. Destefani, S. E. Ulloa, and G. E. Marques, Phys. Rev. B **69**, 125302 (2004).
[16] C. M. Lieber, Nano Lett. **2**, 81 (2002).
[17] B. J. Ohlsson et al. Appl. Phys. Lett. **79**, 3335 (2001). M. T. Björk et al. Nano Lett. **2**, 87 (2002).
[18] M. T. Björk et al. Nano Lett. **4** 1621 (2004).
[19] Y. Wu, R. Fan, and P. Yang, Nano Lett. **2**, 83 (2002).
[20] A. M. Morales and C. M. Lieber, Science **279**, 208 (1998).
[21] P. I. Tamborenea and H. Metiu, Phys. Rev. Lett. **83**, 3912 (1999); P. I. Tamborenea and H. Metiu, Europhys. Lett. **53**, 776 (2001).
[22] P. Zhang and X.-G. Zhao, Phys. Lett. A **271** 419 (2000).
[23] L. Meza-Montes, S. E. Ulloa, and D. Pfannkuche, Physica E **1**, 274 (1998); A. Fendrik, M. J. Sánchez, and P. I. Tamborenea, Phys. Rev. B **63**, 115313 (2001).
[24] C. E. Creffield and G. Platero, Phys. Rev. B **69**, 165312 (2004); Phys. Rev. B **65**, 113304 (2002).
[25] C. F. Destefani, S. E. Ulloa, and G. E. Marques, Phys. Rev. B, accepted for publication.
[26] *Principles of Quantum Mechanics*, R. Shankar (Second Edition, Plenum Press, NY, 1987).
[27] O. Voskoboynikov, C. P. Lee, and O. Tretyak, Phy. Rev. B **63**, 165306 (2001).
[28] V. I. Perel', S. A. Tarasenko, I. N. Yassievich, S. D. Ganichev, V. V. Bel'kov, and W. Prettl, Phys. Rev. B **67**, 201304 (2003).